Supplementary Information for

Structured cyclic peptides that bind the EH domain of EHD1

Alissa J. Kamens,[a] Robyn J. Eisert,[a] Tiffany Corlin,[b] James Baleja,[b] and Joshua A. Kritzer[a]

[a] Department of Chemistry, Tufts University, 62 Talbot Ave., Medford, MA 02155
[b] Department of Developmental, Molecular, and Chemical Biology, Tufts University School of Medicine, 136 Harrison Ave., Boston, MA 02111.

Table of Contents

Protein preparation. The EH domains were prepared from plasmids encoding the EH domain of EHD1 (EHD1-EH) and the second EH domain of Eps15 (Eps15-EH2), as described.[1] The EH domains were expressed in BL21 cells as a glutathione S-transferase (GST) fusion and were purified on a glutathione-agarose column (Gold Biotechnology).[1,2] The EH domains were cleaved from the glutathione-agarose column with thrombin (Sigma Aldrich), and thrombin was removed via a benzamidine-agarose column (Sigma Aldrich). Proteins were dialyzed in buffer (25 mM MOPS, 1 mM $CaCl_2$, pH = 7.0) using 3.5 KDa MWCO dialyzers (Thermo-Scientific) at 4°C.[1] The purity of each protein was verified by SDS-PAGE with a 4-20% SDS gradient gel (Bio-Rad), and all proteins were determined to be >95 % pure (Figure S1A, B). Concentrations were measured by absorbance at 280 nm, using an extinction coefficient of 13980 $M^{-1}cm^{-1}$.

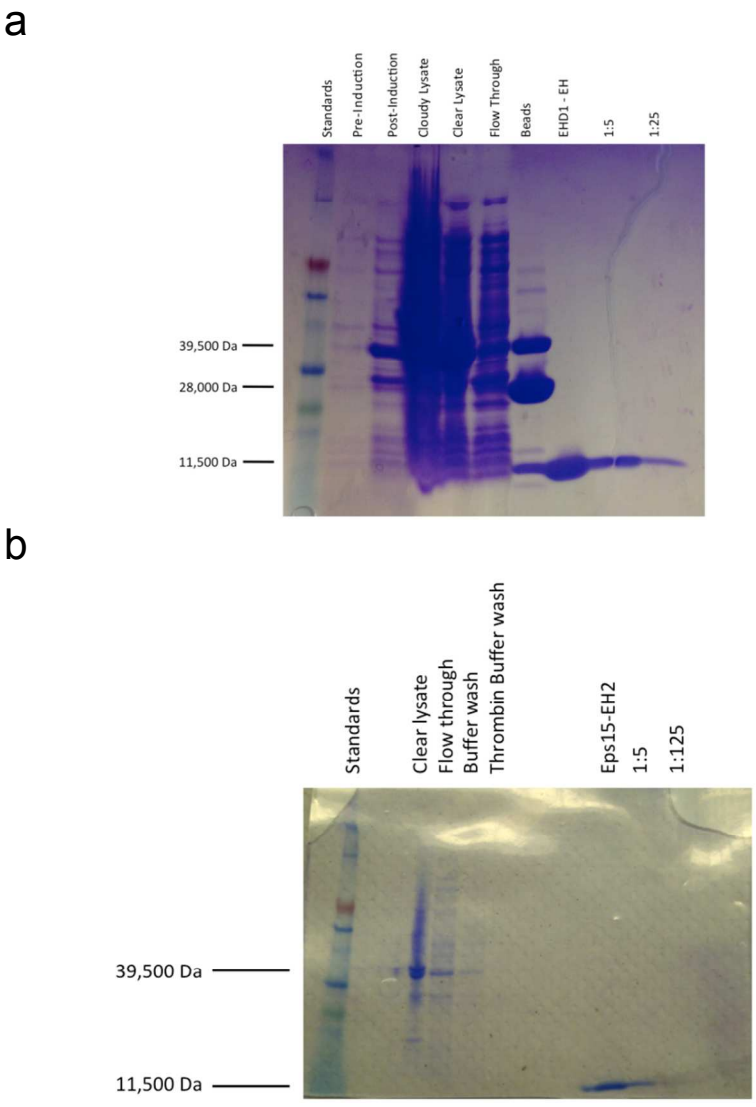

Figure S1. (a) SDS-PAGE of samples from EHD1-EH preparation. (b) SDS-PAGE of samples from Eps15-EH2 preparation. The contents of each lane are listed above the image. Serial dilutions (1:5, 1:25, and 1:125) are shown to verify protein purity.

Peptide synthesis and purification. Materials were purchased from EMD Biosciences, Anaspec and Creosalis. All peptides were synthesized by solid-phase peptide synthesis (SPPS), using standard 9-fluoromethyloxycarbonyl (Fmoc) chemistry. Unless otherwise indicated, all fluoresceinated peptides were labeled on resin by coupling 5(6)-carboxyfluorescein succinimidyl ester. All of the peptides were purified by reverse-phase HPLC (Varian Prostar) on a C18 preparatory scale column and H_2O/CH_3CN with 0.1% trifluoroacetic acid, using a 5-55 % $CH_3CN:H_2O$ gradient over 30 minutes. The peptides were then re-purified on a C18 analytical scale column as needed, until the final product was ≥95% pure. The lyophilized peptides were dissolved in dimethyl sulfoxide to prepare final stock solutions. Concentrations were determined in by absorbance at 274 nm with an extinction coefficient of 1280 $M^{-1}cm^{-1}$ in the assay buffer described below. The concentrations of fluorescently labeled peptides were determined with an extinction coefficient of 77,700 $M^{-1}cm^{-1}$ in 50 mM Tris (pH = 9.0), 150 mM NaCl, and 2.5 mM $CaCl_2$. Retention times are listed for a C18 analytical column and guard column. The peptides' identities were confirmed via ESI (Thermoscientific Finnigan LTQ) or MALDI-TOF (Bruker Microflex) mass spectrometry. Pure peptides were stored as concentrated stocks in dimethylsulfoxide (DMSO).

Table S1. Peptide preparation data. Masses detected by MALDI-TOF unless otherwise noted.

Peptide	Sequence	Retention time (min)	Expected Mass (m/z)	Observed Mass (m/z)
Linear	Ac-YNPFEEGG-$CONH_2$	17.0	952.4	953.4[a]
cNPF1	-YNPFEEGG-	18.0	893.4	894.4[a]
Linear-Flu	(Flu)-ββYNPFEE-$CONH_2$	21.8	1296.5	1297.5[a]
cNPF1-Flu	-YNPFEEGK(Flu)-	23.5	1322.5	1321.2
cNPF2-Flu	-YNPFEEγK(Flu)-	23.2	1349.5	1348.1
cNPF3-Flu	-YNPFEEK(Flu)-	23.1	1265.5	1263.3
cNPF4-Flu	-YNPFEAGK(Flu)-	23.8	1264.5	1262.6
cNPF5-Flu	-YNPFAEGK(Flu)-	23.9	1264.5	1262.9
cNPF6-Flu	-YNPFEQGK(Flu)-	23.0	1321.5	1320.4
cAPA-Flu	-YAPAEEGK(Flu)-	20.1	1203.5	1204.5[a]
cNPF1B	-YNPFEEGK(Ac)-	18.8	1006.4	1004.9
cNPF5	-YNPFAEGK-	19.7[b]	835.4	834.1
cAPA	-YAPAEEGG-	12.3	774.3	775.4[a]

[a] Mass taken by ESI
[b] On analytical C8 column

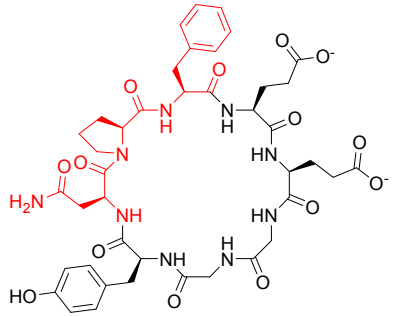

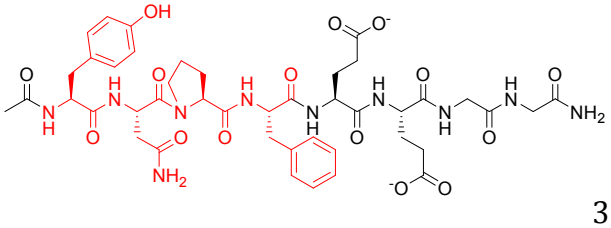

Figure S2. Chemical structures of cNPF1 (top) and the linear NPF peptide (bottom). The NPF motif is shown in red. Structures are shown in their protonation states at pH = 7.0.

Isothermal titration calorimetry. The experiments were performed on a Microcal ITC200 system (GE Healthcare). All proteins and peptides were dialyzed together in 25 mM MOPS, 1 mM $CaCl_2$, and NaCl (as specified) at a pH of 7.0 at 4°C prior to the experiments. Dialyzers had a molecular weight cut-off of 3,500 Da (Thermoscientific Slide-a-lyzer, 0.5-3 mL) for protein dialysis and a molecular weight cut-off of 100-500 Da (Spectrum Labs, Micro Float-a-lyzer dialysis device) for peptide dialysis. ITC experiments were performed at 20°C with stock solutions of 20-50 μM protein and tenfold concentration of peptide. The buffer was verified to be pH=6.8 at the experimental temperature.

Table S2. Binding data from ITC.

Peptide	NaCl (mM)	K_d (μM)	ΔH° (kcal/mol)	ΔS° (cal/mol°)	N	Figure
Linear	0	5.24	-10.1	-10.2	0.959	S3a
		5.65	-9.68	-9.02	1.06	S3b
		5.99	-9.95	-10.0	1.09	S3c
	Average	5.6 ± 0.6	-9.9 ± 0.2	-9.7 ± 0.3	1.04 ± 0.07	N/A
	15	11.06	-10.1	-11.9	1.08	S3d
		9.17	-9.33	-8.77	1.13	S3e
		8.62	-9.06	-7.73	1.06	S3f
		8.54	-9.07	-7.75	1.04	S3g
	Average	9.4 ± 1.2	-9.3 ± 0.5	-9.0 ± 2.0	1.08 ± 0.04	N/A
	150	33.90	-10.6	-15.5	0.951	S3h
		40.00	-12.5	-22.4	0.872	S3i
		33.33	-11.9	-14.3	1.07	S3j
	Average	35.7 ± 3.7	-11.1 ± 1.2	-17.4 ± 4.9	0.96 ± 0.06	N/A
cNPF1	0	1.33	-11.8	-13.3	1.03	S3k
		1.50	-11.7	-13.1	1.04	S3l
		1.51	-11.9	-14.5	1.05	S3m
	Average	1.6 ± 0.3	-11.8 ± 1.3	-13.6 ± 0.8	1.04 ± 0.01	N/A
	15	1.84	-10.6	-9.79	1.17	S3n
		2.61	-12.7	-17.8	0.881	S3o
		2.87	-11.5	-13.9	1.04	S3p
		2.76	-11.9	-15.2	1.01	S3q
	Average	2.5 ± 0.5	-11.7 ± 0.9	-14.2 ±3.3	1.03 ± 0.12	N/A
	150	9.62	-12.0	-17.8	1.04	S3r
		10.74	-11.9	-17.7	1.04	S3s
		9.23	-11.8	-17.1	1.10	S3t
	Average	9.9 ± 0.8	-11.9 ± 0.1	-17.5 ± 0.4	1.06 ± 0.03	N/A

The fourfold improvement in binding affinity for cNPF1 over the linear control suggested that the cyclization of NPF promoted a conformation compatible with target binding. The low affinity of the interaction between the linear peptide and EHD1 at 150 mM salt resulted in a poorer signal-to-noise ratio and larger experimental error. As a result, it was difficult to directly compare the thermodynamic parameters of the linear and cyclic peptides binding to EHD1 at physiological salt. However, the overall trends in the ΔH and ΔS values remained consistent as 15 mM and 0 mM salt, and suggested that the improvement in binding affinity upon cyclization was primarily enthalpic in nature. This supports the hypothesis that the cyclized NPF motif can make more favorable noncovalent interactions with EHD1-EH. Interestingly, the binding

entropy (ΔS) was more thermodynamically favorable for the linear peptide than for cNPF1 at lower salt concentrations. We have previously attributed entropy changes in EH domain binding to differences in water organization around charged residues near the NPF-binding pocket.[1] The small entropic penalty observed for cNPF1 has been seen in other cyclic molecules; evidently, the preorganization of a binding epitope does not always confer entropically favored protein-ligand interactions, and that the entropy of these interactions may be dominated by water organization rather than peptide structure.[3,4,5] The difference in ΔS between linear and cyclic peptides was no longer observed under physiological salt conditions, perhaps because the greater concentration of NaCl lessened the organization of water around the negatively charged side-chains of the ligand and the positively charged side-chains of the protein.

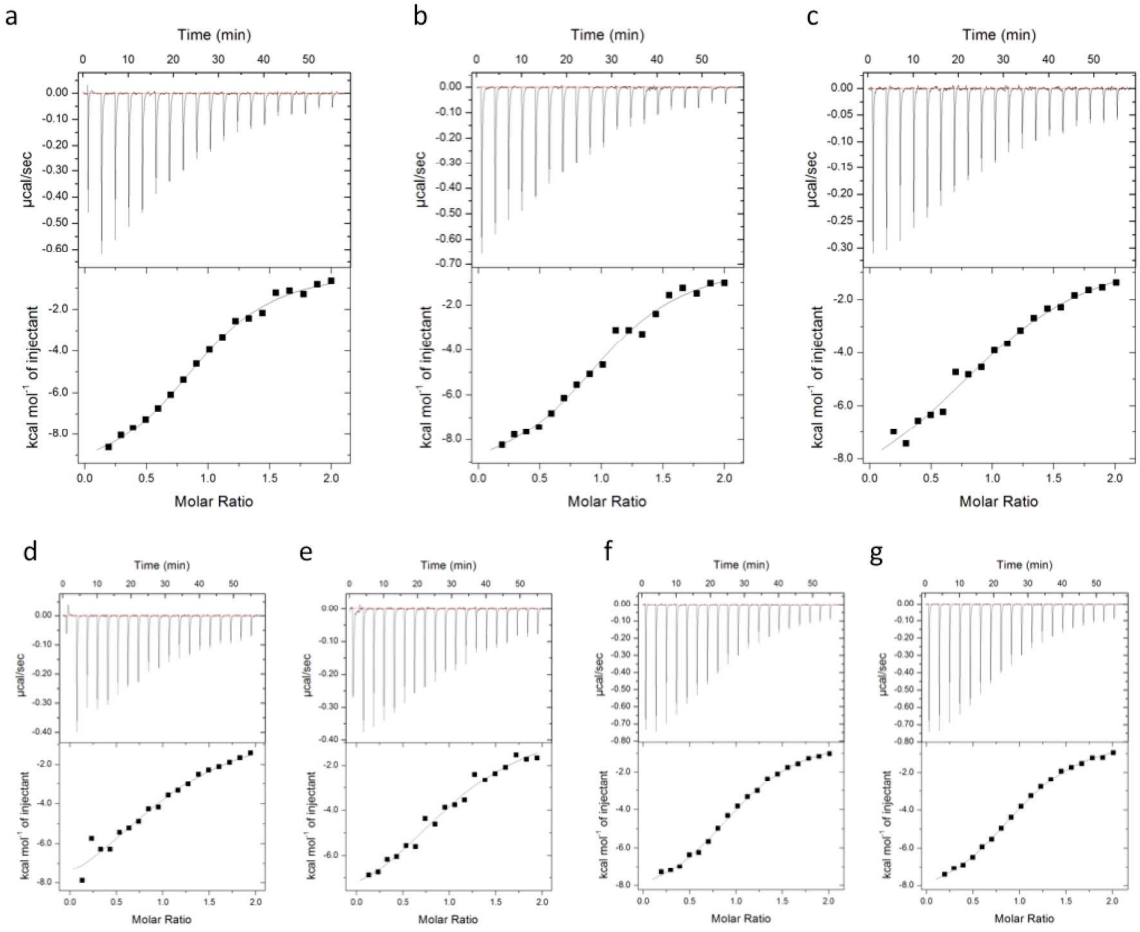

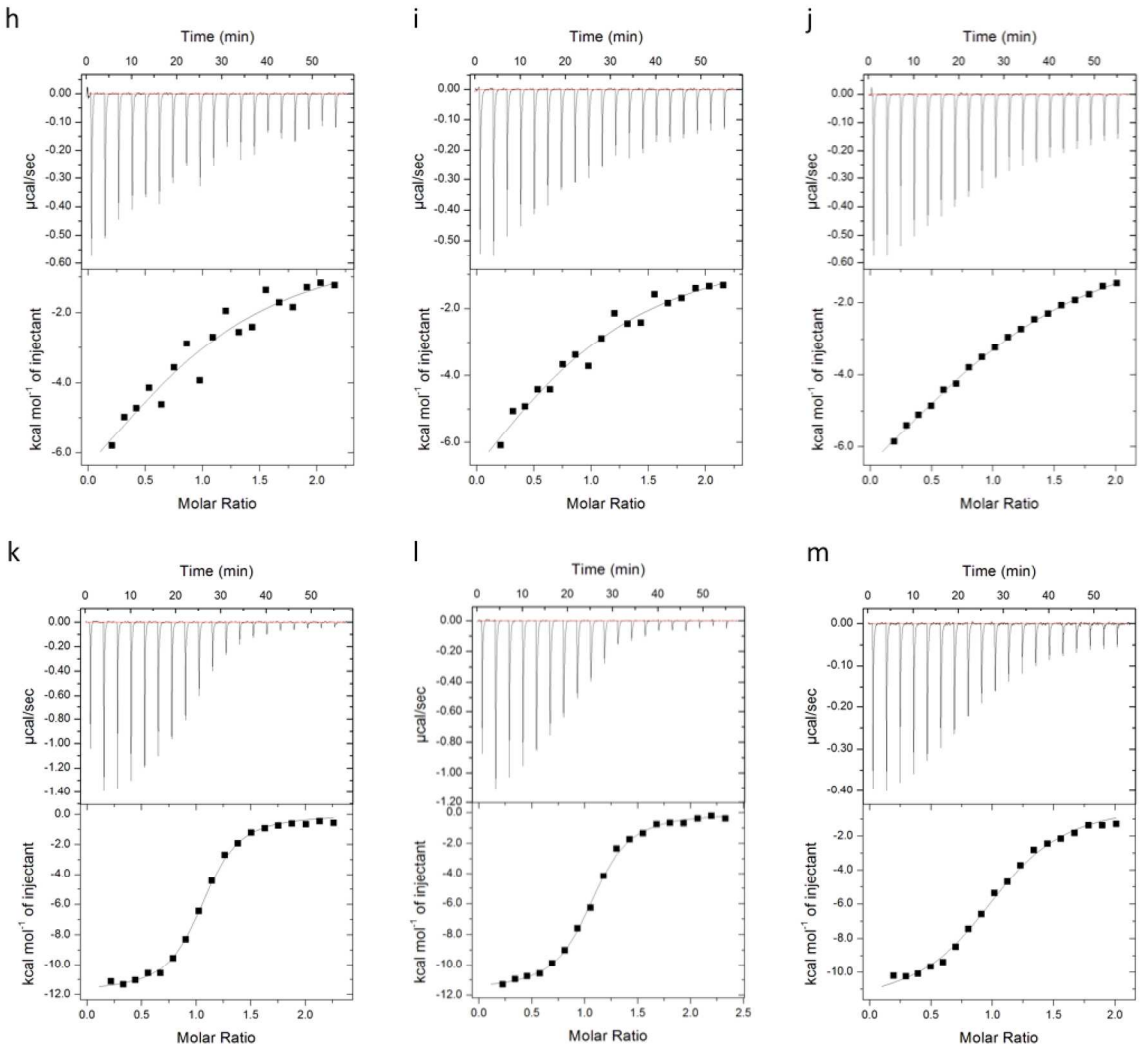
h
i
j
k
l
m
Time (min)
µcal/sec
kcal mol^{-1} of injectant
Molar Ratio

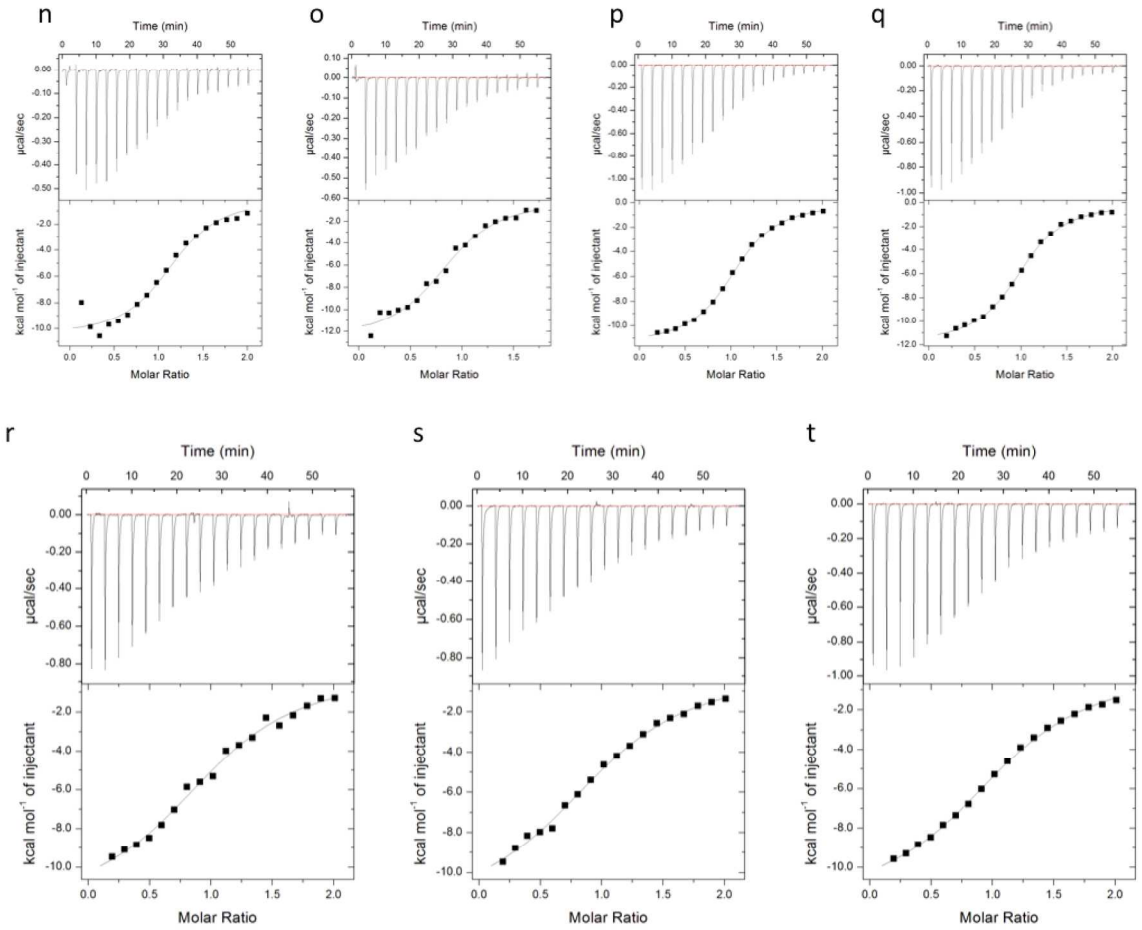

Figure S3. Raw data from ITC experiments. (a-c) ITC data from experiments with the linear control with no NaCl. (d-g) ITC data from experiments with the linear control at 15 mM NaCl. (h-j) ITC data from experiments with the linear control at 150 mM NaCl. (k-m) ITC data from experiments with cNPF1 and no NaCl. (n-q) ITC data from cNPF1 experiments at 15 mM NaCl. (r-t) ITC data from experiments with cNPF1 at 150 mM NaCl.

Fluorescence polarization (FP) assays. All FP experiments were performed in flat-bottom, black 384 well plates (Corning). The assay buffer (25 mM MOPS, and 1 mM $CaCl_2$ at a pH of 7.0 at 4^{o}C) had a final NaCl concentration of either 15 or 150 mM as needed. Each experiment also had a final concentration of 1.5% DMSO and 0.1% Tween-20, which were added along with the probe. The buffer was verified to be pH=6.8 at 20°C. Each probe was incubated at a final concentration of 100 nM at room temperature with varying concentrations of EHD1-EH or Eps15-EH2. The plates were spun at 1,600 G at 20°C after the addition of the probe. Fluorescence polarization was measured 1 hour after the addition of the probe, and again at 4 hours after addition of the probe (Tecan F200 Pro). No difference in the data was detected between 1 and 4 hours, and 1-hour data was used for curve fitting. K_d curve fits were derived from first principles, and calculated using non-linear regression (Kaleidagraph, Synergy Software, Equation 1). The data obtained from the 150 mM NaCl experiments were fit by assuming the upper bounds observed for each probe at 15 mM NaCl. Three or more independent trials were performed on each probe, under both sets of salt conditions.

(1) $$P = P_F + (P_B - P_F) \times \frac{L_T + K_d + R_T - \sqrt{[(L_T + K_d + R_T)^2 - 4L_T R_T]}}{2}$$

P = experimental polarization value, P_F = polarization of free ligand, P_B = polarization of bound ligand, L_T = total ligand concentration, K_d = dissociation constant, R_T = total concentration of protein.

Table S3. Data from FP binding assays. K_d values were obtained from the curve fits shown in Figures 1 and S4.

Peptide	K_d (μM) 15 mM NaCl	K_d (μM) 150 mM NaCl
Lin-Flu	6.9 ± 0.6	31.4 ± 0.5
cNPF1-Flu	3.3 ± 0.3	16.8 ± 0.1
cNPF2-Flu	4.5 ± 0.3	20.5 ± 0.3
cNPF3-Flu	11.3 ± 1.0	57.8 ± 0.2
cNPF4-Flu	17.4 ± 0.1	46.7 ± 0.9
cNPF5-Flu	8.7 ± 0.9	28.3 ± 0.3
cNPF6-Flu	12.8 ± 0.8	34.0 ± 0.3
cAPA-Flu	> 67	Not determined

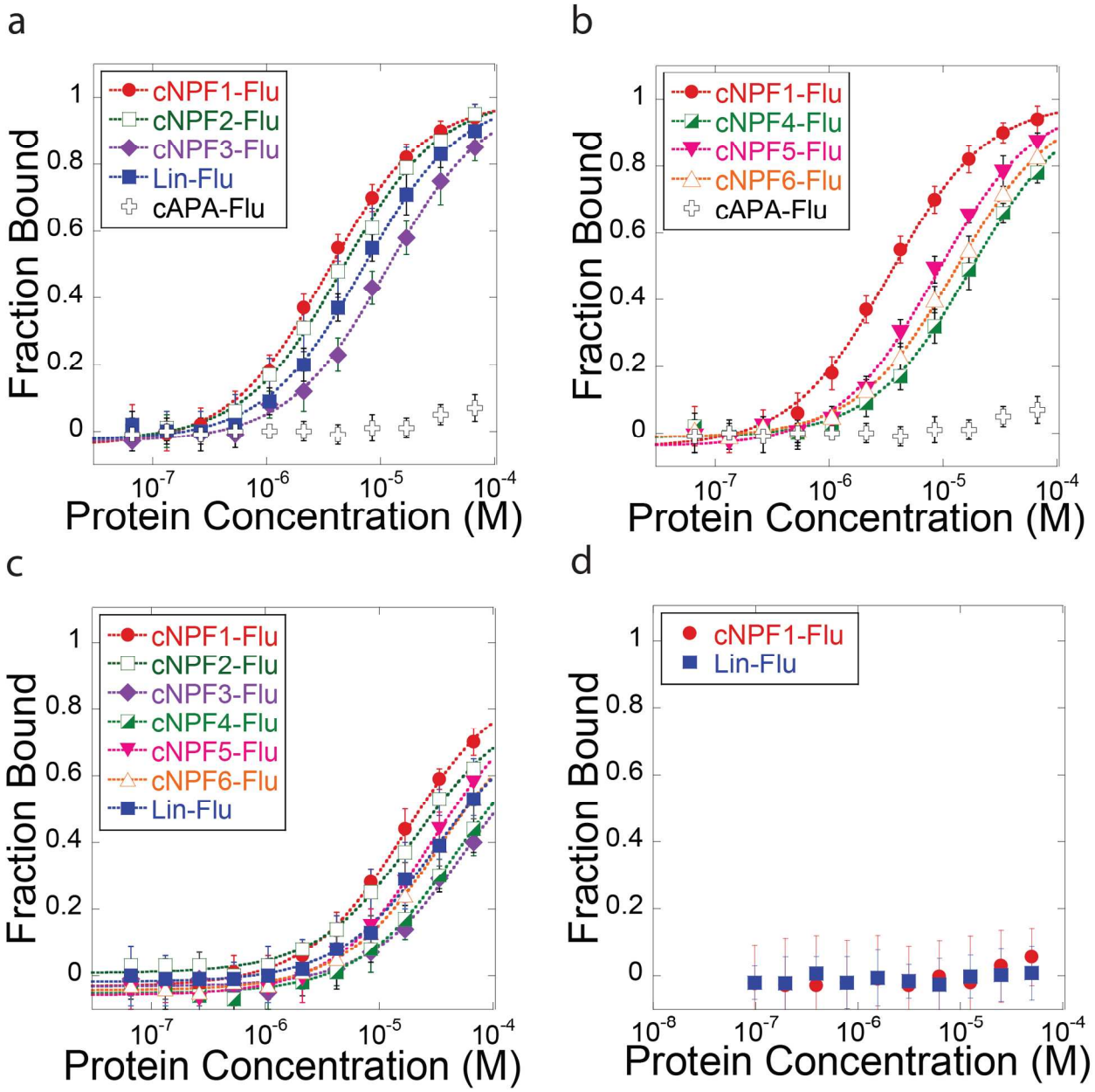

Figure S4. FP direct binding data. Identical data to Figure 1a are reproduced here, separated into two plots that compare different macrocycle sizes (a) and different substitutions for the negatively charged side chains (b). Data from similar direct binding assays at 150 mM NaCl are shown in (c), with curve fits shown. Curves for the data in (c) were fitted using the upper polarization limits from the data in (a) and (b) in order to extract K_d values solely for comparison among the different peptides at physiological salt. (d) Direct binding experiments with Eps15-EH2. Eps15 experiments were performed with 1mM DL-dithiothreitol (Sigma Aldrich). Error bars show standard deviation from three to four independent trials. Binding experiments with Eps15-EH2 (d) were done in duplicate.

Circular dichroism. EHD1-EH and Eps15-EH2 was dialyzed at 4°C in 10 mM sodium phosphate buffer at pH = 7.0 with 1 mM $CaCl_2$ and 1 mM dithiothreitol. CD was performed at room temperature (Jasco J-715 circular dichroism spectropolarimeter) with EHD1-EH at 40.3 μM and Eps15-EH2 at 35.5 μM. Spectra were taken from 190 nm to 260 nm at 1nm intervals.

a

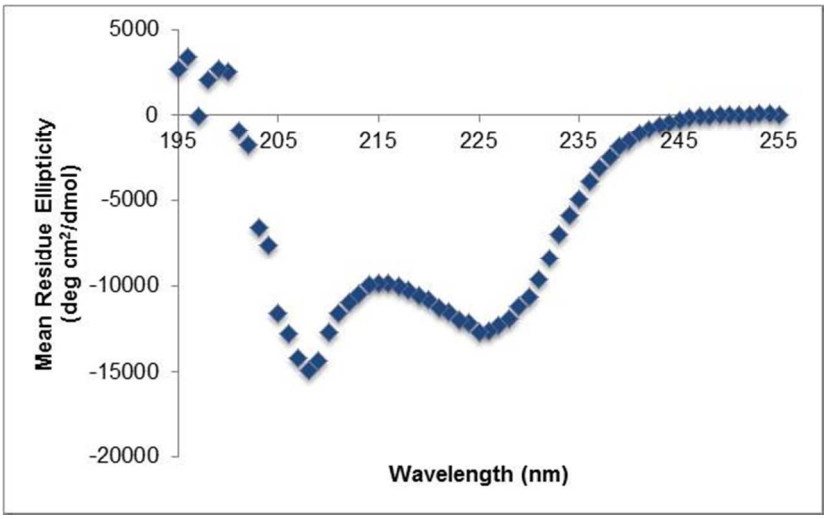

b

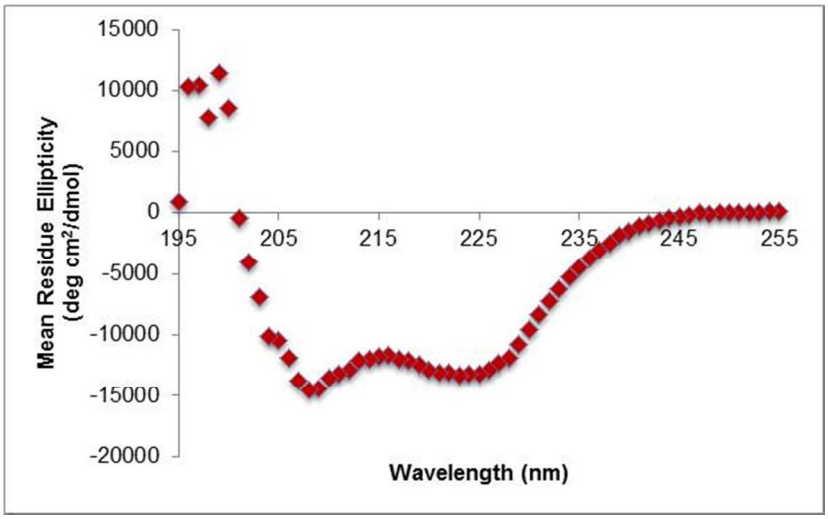

Figure S5. CD spectra of EHD1-EH (a) and Eps15-EH2 (b). The spectra for both proteins are consistent with predominantly alpha-helical secondary structure, as expected for EH domains. These results indicate that the proteins were properly folded, and that lack of binding affinity for Eps15-EH2 by cNPF1-flu results from genuine selectivity among EH domains.

Fluorescence polarization competition assays. All experiments were performed in flat-bottom, black 384 well plates (Corning). The assay buffers were prepared at 4°C with 25 mM MOPS with pH = 7.0, 1 mM $CaCl_2$, and 15 mM NaCl. The experiments were performed at room temperature, at which MOPS was verified to have a pH of 6.8. Each experiment also had a final concentration of 1.5% DMSO and 0.1% Tween-20, which were added along with the probe. Each inhibitor was added and to EHD1-EH, spun at 1,600 G , and incubated at room temperature for 30 minutes. The fluorescent probes were then added to the mixture so that the final concentration of probe was 100 nM and the final concentration of EHD1-EH was 20 μM. The plates were spun at 1,600 G at 20°C after the addition of the probe. No difference in the data was detected between 1 and 4 hours, and 1-hour data was used for curve fitting. The fluorescence polarization was measured at 1 hour and 4 hours after the addition of the probe. The IC_{50} curve fits were calculated with a non-linear regression software (Kaleidagraph, Synergy Software, Equation 2). No deviation in fluorescence signal was observed up to DMSO concentrations of 10%.

(2) $$P = P_F + \frac{(P_B - P_F)}{(1+10^{[X-Log(IC_{50})]})}$$

P = measured polarization, P_F = polarization of free probe, P_B = polarization of fully bound probe, X = concentration of inhibitor, IC_{50} = half-maximal inhibitory concentration.

NMR Spectroscopy. The NMR spectra were collected on a Bruker Avance 600 MHz spectrometer. The linear NPF peptide and cNPF1 were at concentrations of 1.2 mM and 4.9 mM, respectively, as determined by absorbance at 274 nm with an extinction coefficient of 1280 M^{-1} cm^{-1}. Both peptides were dissolved in 10 mM deuterated imidazole, 10 mM NaCl, 10 mM 4,4-dimethyl-4-silapentane-1-sulfonic acid (DSS) and 0.02% NaN_3 in a 10% D_2O/90% H_2O solution, which was adjusted to a pH between 5.6 and 5.9. A temperature series of ^1H 1D spectra for linear NPF and cNPF1 were collected in 5 °C increments from 5 °C to 25 °C. A total correlation spectroscopy (TOCSY) was collected with a mixing time of 40 ms and a rotating-frame nuclear Overhauser effect correlation spectroscopy (ROESY) was collected at a mixing time of 250 ms at 5 °C. Additionally, a ^{13}C heteronuclear single-quantum correlation spectroscopy (HSQC) and a nuclear Overhauser effect correlation specrescopy (NOESY) with a mixing time of 200 ms were taken at 5 °C for cNPF1. Proton assignments were made according to standard homonuclear methods.[6] Distance restraints, dihedral restraints, hydrogen bond restraints, and both carbon and hydrogen chemical shifts were used in CNSSolve Version 1.3 for structure determination. Restraints were refined with CcpNMR Analysis Version 2.2 and structures were validated with CING through CcpNMR.

Table S4. ^{1}H chemical shifts for cNPF1 and linear NPF peptide, and carbon chemical shifts for cNPF1 determined from ^{13}C-HSQC.

cNPF1	*NH*	*HA*	*HB*	*HG*	*HD*	*HE*
Y1	8.46	4.46	3.12/2.91		7.13	6.85
N2	8.08	4.18	2.72/2.67		7.90/7.13	
P3		4.49	2.05/1.42	1.86/1.76	3.81/3.59	
F4	8.30	4.49	3.39/3.10		7.26	7.38
E5	7.66	4.62	2.11/1.86	2.25/2.23		
E6	8.94	4.16	2.03	2.29		
G7	8.87	4.26/3.78				
G8	8.07	3.81/3.96				
Linear NPF	*NH*	*HA*	*HB*	*HG*	*HD*	*HE*
Y1	8.36	4.49	2.99/2.87		7.09	6.79
N2	8.49	4.92	2.82/2.62		7.76/7.10	
P3		4.21	2.14/1.63	1.85	3.64/3.40	
F4	8.02	4.59	3.23/3.02		7.28	6.79
E5	7.84	4.26	2.02/1.90	2.22		
E6	8.58	4.24	2.08/1.98	2.30		
G7	8.75	4.01				
G8	8.38	3.91				

cNPF1	*CA*	*CB*	*CG*	*CD*	*CE*
Y1	59.03	38.45			
N2		39.27			
P3	64.15	31.80	27.31	50.68	
F4	58.01	37.98			
E5	54.75	32.20		36.06	
E6	57.80	31.75		35.92	
G7	45.22				
G8	45.26				

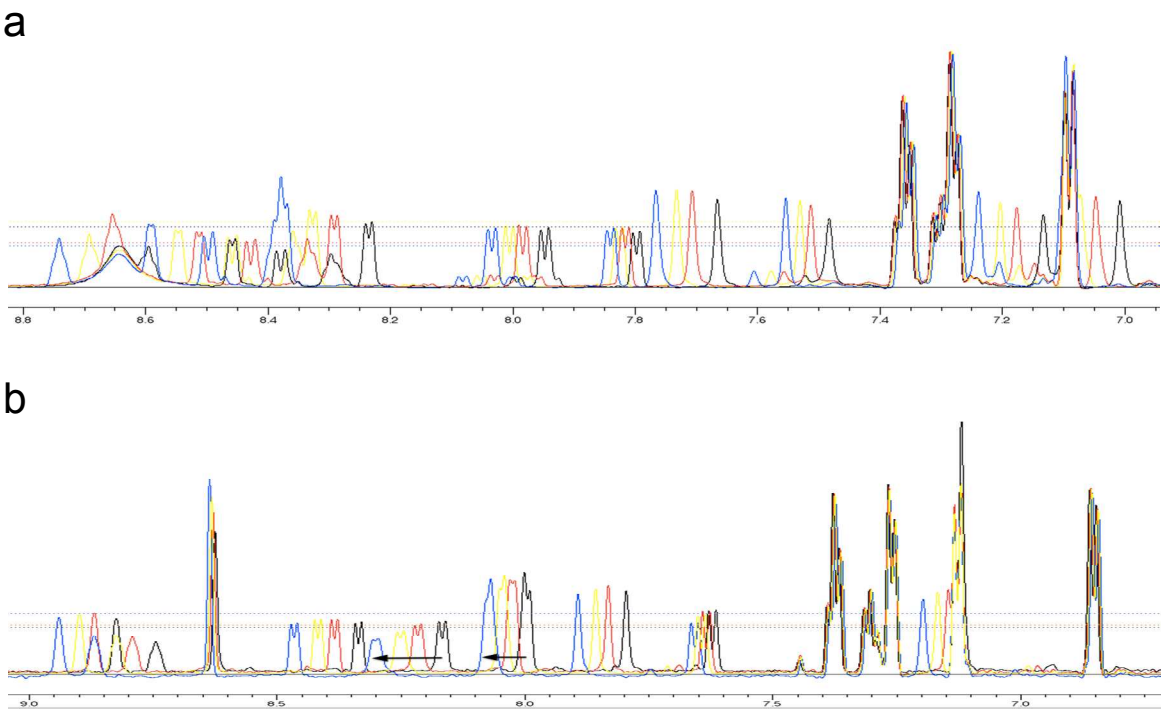

Figure S6. Temperature dependence of amide proton line shapes. a) Temperature series of the amide region of ^{1}H spectra of the linear NPF peptide at 5^{o}C (blue), 10^{o}C (yellow), 15^{o}C (red), and 20^{o}C (black). b) Temperature series of the amide region of ^{1}H spectra of cNPF1 at 5^{o}C (blue), 10^{o}C (yellow), 15^{o}C (red), and 20^{o}C (black). The black arrows at 7.9ppm and 8.3ppm indicate the asparagine and phenylalanine amide peaks, respectively, which are broadening due to their involvement in a hydrogen bond within the NPF motif.

Table S5. NMR structural data and refinement statistics.

	linear NPF peptide	cNPF1
Experimental restraints		
Distance restraints from NOEs	64	135
Dihedral angle restraints	0	3
Hydrogen bond restraints	0	2
Total no. of experimental restraints	64	140
Rms deviations from experimental data		
Average distance restraint violation (Å)	0.0 ± 0.0	0.0 ± 0.0
Dihedral restraint violations > 5°	0.0 ± 0.0	0.0 ± 0.0
Rms deviations from ideal stereochemistry		
Bonds (Å)	0.0046 ± 0.00058	0.0046 ± 0.00011
Angles (deg)	0.4354 ± 0.0247	0.6272 ± 0.0094
Impropers (deg)	0.3822 ± 0.0149	0.5149 ± 0.0232
Ramachandran analysis of the structures		
Residues in favored regions	72.5%	50.0%
Residues in additionally allowed regions	27.5%	50.0%
Residues in disallowed regions	0.0%	0.0%
Lennard-Jones potential energies		
Ensemble average (kcal/mol)	27.30 ± 2.9	43.98 ± 0.8
Coordinate precision (Å)		
Backbone	0.816 ± 0.3701	0.048 ± 0.1085
All heavy atoms	1.343 ± 0.4809	0.556 ± 0.2674

Table S6. Distance Restraints for the linear NPF peptide.

Restraint	Resonances						Value (Å)	Upper Limit	Lower Limit
1	residue	2	HA	residue	2	HN	2.613	3.136	2.090
2	residue	2	HA	residue	2	HB1	2.777	4.177	1.377
3	residue	2	HA	residue	2	HB2	3.032	4.432	1.632
4	residue	2	HB1	residue	2	HN	2.771	3.325	2.217
5	residue	2	HB2	residue	2	HN	2.729	3.275	2.183
6	residue	2	HD#	residue	2	HB2	2.480	4.976	0.000
7	residue	2	HD#	residue	2	HB1	2.332	4.798	0.000
8	residue	2	HD#	residue	2	HA	2.324	4.789	0.000
9	residue	2	HE#	residue	4	HB2	3.198	5.838	0.558
10	residue	3	HN	residue	3	HB1	3.058	3.670	2.446
11	residue	3	HN	residue	3	HB2	2.974	3.569	2.379
12	residue	3	HN	residue	3	HA	2.717	3.260	2.174
13	residue	3	HB1	residue	3	HA	2.707	3.807	1.607
14	residue	3	HB2	residue	3	HA	2.777	3.777	1.777
15	residue	3	HB1	residue	3	HD21	2.800	3.560	2.040
16	residue	3	HB2	residue	3	HD21	3.028	3.834	2.222
17	residue	3	HD22	residue	3	HA	3.363	4.036	2.690
18	residue	3	HN	residue	2	HA	2.247	2.696	1.798
19	residue	4	HA	residue	4	HB1	3.048	4.748	1.348
20	residue	4	HA	residue	4	HB2	2.473	4.073	0.873
21	residue	4	HD1	residue	4	HB1	3.736	6.483	0.989
22	residue	4	HD1	residue	4	HB2	3.385	6.062	0.708
23	residue	4	HG1	residue	4	HA	3.765	5.518	2.012
24	residue	4	HD1	residue	3	HA	2.221	2.665	1.777
25	residue	4	HD1	residue	2	HE#	3.296	5.955	0.637
26	residue	4	HD2	residue	5	HD#	3.251	5.901	0.601
27	residue	4	HD2	residue	3	HA	2.122	2.524	1.698
28	residue	5	HN	residue	5	HA	2.674	3.209	2.139
29	residue	5	HN	residue	5	HB1	3.129	4.255	2.003
30	residue	5	HN	residue	5	HB2	2.641	3.669	1.613
31	residue	5	HA	residue	5	HD#	2.290	4.748	0.000
32	residue	5	HB1	residue	5	HA	3.275	4.575	1.975
33	residue	5	HB2	residue	5	HA	3.037	4.337	1.737
34	residue	5	HB1	residue	5	HD#	2.436	4.923	0.000
35	residue	5	HB2	residue	5	HD#	2.391	4.869	0.000
36	residue	5	HN	residue	4	HB1	3.237	3.884	2.590
37	residue	5	HN	residue	4	HA	2.453	2.944	1.962
38	residue	5	HN	residue	4	HD2	3.046	3.655	2.437
39	residue	6	HN	residue	6	HA	2.799	3.359	2.239
40	residue	6	HN	residue	6	HB1	2.868	3.742	1.994
41	residue	6	HN	residue	6	HB2	3.210	4.152	2.268
42	residue	6	HN	residue	6	HG1	3.121	3.745	2.497
43	residue	6	HA	residue	6	HG1	2.935	3.522	2.348
44	residue	6	HA	residue	6	HB1	2.912	4.012	1.812
45	residue	6	HA	residue	6	HB2	2.960	4.060	1.860
46	residue	6	HN	residue	5	HA	2.385	2.862	1.908
47	residue	7	HN	residue	7	HA	2.265	2.718	1.812
48	residue	7	HN	residue	7	HB1	2.892	3.870	1.914
49	residue	7	HN	residue	7	HB2	3.259	4.779	1.739
50	residue	7	HN	residue	7	HG#	3.421	5.105	1.737
51	residue	7	HA	residue	7	HB1	2.893	3.993	1.793
52	residue	7	HA	residue	7	HB2	2.907	4.007	1.807
53	residue	7	HG#	residue	7	HA	3.080	4.696	1.464
54	residue	8	HN	residue	8	HA1	2.748	3.498	1.998
55	residue	8	HN	residue	8	HA2	2.930	3.716	2.144
56	residue	8	HN	residue	6	HA	2.468	2.962	1.974
57	residue	9	HN	residue	9	HA1	2.417	3.817	1.017
58	residue	9	HN	residue	9	HA2	3.336	4.836	1.836
59	residue	9	HN	residue	7	HA	3.205	3.846	2.564

Table S7. Distance Restraints for cNPF1.

Restraint	Resonances						Value (Å)	Upper Limit	Lower Limit
1	residue	1	HN	residue	1	HB1	2.313	3.426	1.200
2	residue	1	HN	residue	1	HB2	2.610	4.032	1.188
3	residue	1	HA	residue	1	HB1	2.719	3.863	1.575
4	residue	1	HA	residue	1	HB2	2.837	4.104	1.570
5	residue	1	HA	residue	1	HD#	2.490	4.988	0.000
6	residue	1	HE#	residue	1	HA	3.427	6.112	0.742
7	residue	1	HN	residue	1	HA	2.520	3.024	2.016
8	residue	1	HB1	residue	1	HD#	2.330	4.796	0.000
9	residue	1	HB2	residue	1	HD#	2.364	4.837	0.000
10	residue	1	HE#	residue	1	HB1	3.329	6.095	0.563
11	residue	1	HE#	residue	1	HB2	3.476	6.271	0.681
12	residue	1	HN	residue	1	HD#	2.909	5.491	0.327
13	residue	1	HB1	residue	2	HN	2.879	3.605	2.153
14	residue	1	HB2	residue	2	HN	2.939	4.939	2.351
15	residue	1	HB2	residue	2	HD22	3.898	5.128	2.668
16	residue	1	HB1	residue	2	HD22	3.635	5.112	2.158
17	residue	1	HA	residue	2	HN	2.904	3.585	2.223
18	residue	1	HN	residue	2	HN	2.128	2.536	1.702
19	residue	1	HN	residue	5	HB1	3.683	5.020	2.346
20	residue	1	HN	residue	5	HB2	3.774	5.179	2.369
21	residue	1	HN	residue	8	HA2	2.583	3.200	1.966
22	residue	1	HN	residue	8	HA1	2.320	3.284	1.356
23	residue	2	HB#	residue	1	HD#	3.185	6.022	0.348
24	residue	2	HB#	residue	2	HD22	2.658	3.790	1.526
25	residue	2	HB2	residue	2	HD21	3.034	5.141	1.927
26	residue	2	HB1	residue	2	HD21	3.318	4.882	1.754
27	residue	2	HB1	residue	2	HD22	2.695	3.834	1.556
28	residue	2	HB#	residue	2	HD22	2.319	3.783	0.855
29	residue	2	HN	residue	2	HB#	2.375	3.850	0.900
30	residue	2	HA	residue	2	HD21	3.315	4.528	2.102
31	residue	2	HA	residue	2	HD22	3.553	5.024	2.082
32	residue	2	HN	residue	2	HB1	2.730	3.526	1.934
33	residue	2	HN	residue	2	HB2	2.710	3.752	1.668
34	residue	2	HN	residue	2	HA	2.455	2.946	1.964
34	residue	2	HB2	residue	2	HA	2.664	3.897	1.431
35	residue	2	HB1	residue	2	HA	2.881	4.157	1.605
36	residue	2	HD22	residue	2	HD21	1.720	1.920	1.376
37	residue	2	HB2	residue	5	HN	3.975	6.270	2.680
38	residue	2	HB1	residue	5	HN	3.436	4.973	2.099
39	residue	2	HN	residue	5	HG#	3.626	5.351	1.901
40	residue	3	HD2	residue	2	HA	2.408	3.360	1.456
41	residue	3	HD1	residue	2	HA	2.232	3.278	1.186
42	residue	3	HD2	residue	2	HB1	2.612	3.824	1.340
43	residue	3	HD2	residue	2	HB2	2.789	3.947	1.631
44	residue	3	HG1	residue	2	HB#	3.302	4.962	1.642
45	residue	3	HD1	residue	2	HB1	3.189	4.077	2.301
46	residue	3	HD1	residue	2	HB2	3.201	4.041	2.361
47	residue	3	HG2	residue	3	HA	3.671	4.905	2.437
48	residue	3	HG1	residue	3	HA	3.128	4.254	2.002
49	residue	3	HD1	residue	3	HB1	3.251	4.101	2.401
50	residue	3	HD2	residue	3	HB1	3.448	4.338	2.558
51	residue	3	HG2	residue	3	HB2	2.479	2.975	1.983
52	residue	3	HB2	residue	3	HB1	2.356	3.827	1.885
53	residue	3	HG2	residue	3	HD2	2.384	3.461	1.307
54	residue	3	HG1	residue	3	HD2	2.711	3.853	1.569
55	residue	3	HA	residue	3	HB2	2.639	3.667	1.611
56	residue	3	HG1	residue	3	HB2	2.597	3.116	2.078

57	residue	3	HD2	residue	3	HB2	3.086	4.003	2.169
58	residue	3	HG2	residue	3	HD1	2.804	3.365	2.243
59	residue	3	HA	residue	3	HB1	2.208	3.650	0.766
	residue	6	HB1	residue	3	HA			
60	residue	3	HG1	residue	3	HD1	2.414	3.447	1.381
61	residue	3	HD2	residue	4	HN	3.145	4.374	1.916
62	residue	3	HD1	residue	4	HN	3.756	5.157	2.355
63	residue	3	HD2	residue	4	HD#	3.436	6.223	0.649
64	residue	3	HG2	residue	4	HN	3.518	4.772	2.264
65	residue	4	HB2	residue	2	HD22	3.830	7.096	0.564
66	residue	4	HB2	residue	2	HD21	3.687	5.924	1.450
67	residue	4	HD#	residue	2	HB2	3.450	6.240	0.660
68	residue	4	HN	residue	2	HB1	3.572	4.586	2.558
69	residue	4	HN	residue	2	HB2	3.730	6.576	2.884
70	residue	4	HN	residue	3	HB2	3.334	4.401	2.267
71	residue	4	HD#	residue	3	HB2	2.983	5.630	0.336
72	residue	4	HN	residue	3	HA	2.338	3.536	1.140
73	residue	4	HN	residue	4	HA	2.432	3.068	1.796
74	residue	4	HB1	residue	4	HA	3.003	4.304	1.702
75	residue	4	HB2	residue	4	HA	2.805	4.066	1.544
76	residue	4	HB2	residue	4	HN	2.624	3.699	1.549
77	residue	4	HB1	residue	4	HN	3.127	4.252	2.002
78	residue	4	HB2	residue	4	HE#	3.307	6.268	0.346
79	residue	4	HB1	residue	4	HE#	3.618	6.642	0.594
80	residue	4	HD#	residue	4	HB2	2.248	4.898	-0.402
81	residue	4	HD#	residue	4	HB1	2.442	5.130	-0.246
82	residue	4	HD#	residue	4	HN	3.055	5.666	0.444
83	residue	4	HD#	residue	4	HA	2.386	4.863	-0.091
84	residue	4	HB1	residue	5	HN	3.337	4.204	1.137
85	residue	4	HB2	residue	5	HN	3.147	3.976	0.947
86	residue	4	HA	residue	5	HN	2.878	3.704	2.252
87	residue	4	HN	residue	5	HN	2.401	2.931	1.871
88	residue	5	HG#	residue	2	HD21	3.393	5.172	1.614
89	residue	5	HG#	residue	2	HD22	3.554	5.365	1.743
90	residue	5	HB1	residue	2	HN	3.062	3.874	2.250
91	residue	5	HB2	residue	2	HN	3.127	5.862	2.392
92	residue	5	HB1	residue	2	HD21	3.609	6.331	2.887
93	residue	5	HB1	residue	2	HD22	3.941	6.729	3.153
94	residue	5	HB1	residue	2	HB1	3.201	4.441	1.961
95	residue	5	HB1	residue	2	HB2	3.161	4.443	1.879
96	residue	5	HG#	residue	2	HD22	3.877	5.652	2.102
97	residue	5	HG#	residue	2	HD21	3.587	5.304	1.870
98	residue	5	HN	residue	3	HA	3.260	4.312	2.208
99	residue	5	HB2	residue	5	HN	2.850	3.520	2.180
100	residue	5	HA	residue	5	HG#	3.569	5.283	1.855
101	residue	5	HB2	residue	5	HA	2.620	4.044	1.196
102	residue	5	HB1	residue	5	HA	3.016	4.519	1.513
103	residue	5	HN	residue	5	HG#	2.984	4.581	1.387
104	residue	5	HN	residue	5	HG#	2.868	4.442	1.294
105	residue	5	HB1	residue	5	HN	2.487	3.034	1.940
106	residue	5	HA	residue	5	HN	2.465	2.958	1.972
107	residue	5	HA	residue	5	HG#	2.638	4.216	1.060
108	residue	5	HA	residue	6	HN	2.600	3.570	1.630
109	residue	5	HB1	residue	6	HN	3.107	4.078	2.136
110	residue	5	HB2	residue	6	HN	3.098	4.168	2.028
111	residue	5	HG#	residue	8	HN	3.583	5.300	1.866
112	residue	6	HN	residue	2	HA	3.330	5.896	0.764
113	residue	6	HB2	residue	3	HA	2.148	3.576	0.718
	residue	6	HA	residue	3	HB1			
	residue	3	HA	residue	3	HB1			
	residue	6	HB2	residue	6	HA			
114	residue	6	HG#	residue	3	HA	3.652	5.482	1.822

115	residue	6	HB2	residue	6	HN	2.332	4.048	0.616
116	residue	6	HN	residue	6	HG#	2.915	4.498	1.332
117	residue	6	HB#	residue	6	HN	2.145	3.570	0.716
118	residue	6	HN	residue	6	HG1	3.434	4.371	2.497
119	residue	6	HN	residue	6	HG2	3.326	4.091	2.561
120	residue	6	HA	residue	6	HN	2.520	3.024	2.016
121	residue	6	HA	residue	6	HG1	3.433	4.420	2.446
122	residue	6	HN	residue	5	HN	3.375	6.050	2.700
123	residue	6	HA	residue	7	HN	2.600	3.470	1.730
124	residue	6	HG#	residue	7	HN	3.432	5.118	1.746
125	residue	6	HB#	residue	7	HN	2.853	4.424	1.282
126	residue	6	HA	residue	8	HN	3.468	4.162	2.774
127	residue	7	HA1	residue	7	HA2	2.031	2.342	1.625
128	residue	7	HA1	residue	7	HN	2.053	2.766	1.342
129	residue	7	HA2	residue	7	HN	2.545	3.254	1.836
130	residue	8	HN	residue	7	HN	2.476	3.971	1.981
131	residue	8	HN	residue	7	HA1	3.181	3.817	2.545
132	residue	8	HN	residue	7	HA2	2.813	3.376	2.250
133	residue	8	HA1	residue	8	HN	2.928	4.214	1.642
134	residue	8	HA2	residue	8	HN	2.103	3.286	0.982

References

[1] Henry, G.; Corrigan, D.; Dineen, J.; Baleja, J. *Biochemistry*, **2010**, *49*, 3381-3392.

[2] Kim, S.; Dubelman, A.; Goonesekera, S.; Feig, L.; Baleja,J. *J. Biomolec. NMR*, **2000**, *18*, 367-368.

[3] DeLorbe, J. E.; Clements, J. H.; Teresk, M.G.; Benfield, A. P.; Plake, S. R.; Millspaugh, L. E.; Martin, S. F. *JACS*, **2009**, *131*, 16758-16770.

[4] DeLorbe, J. E.; Clements, J. H.; Whiddon, B. B.; Martin, S. F. *ACS Med. Chem. Lett.* **2010**, *1*, 448-452.

[5] Udugamasooriya, D. G.; Spaller, M. R. *Biopolymers*, **2008**, *89*, 653-667.

[6] Wüthrich K. NMR of Proteins and Nucleic Acids. New York: Wiley; 1986.